Fluorescent Probes

DOI: 10.1002/anie.201206446

Oligothiophene Amphiphiles as Planarizable and Polarizable Fluorescent Membrane Probes**

*Andrea Fin, Andreas Vargas Jentzsch, Naomi Sakai, and Stefan Matile**

During cooking, lobsters change their color from dark blue to bright red, because their astaxanthin chromophore is both deplanarized and depolarized when the surrounding β-crustacyanine β barrel is thermally denatured.[1] Similar processes contribute to the chemistry of vision.[2] We wondered whether or not these lessons from nature could be helpful for the discovery of conceptually new fluorescent membrane probes. In this initial report on the topic, we show that the coupling of polarization and planarization of oligothiophene amphiphiles is compatible with the detection of membrane fluidity and membrane potentials.

The separate topics that are bundled together in this study have been explored extensively. So-called push–pull fluorophores, that is, fluorophores that are equipped with a π donor at one end and a π acceptor at the other, are the leading membrane probes to detect microdomains and membrane potentials.[3–5] Examples include the families around laurdan, Nile red, *p*-oligophenyls[4] as well as pioneering push–pull oligothiophenes from the Loew research group.[5] Push–pull oligothiophenes have further attracted interest for applications in nonlinear optics (NLO), photovoltaics, and biology.[6–8] The deplanarization of push–pull fluorophores in the excited state received much attention in the context of molecular rotors.[8,9] These fluorophores are used as viscosity sensors and, in pioneering studies, also to report on the fluidity of lipid bilayer membranes.[9] The planarization of push–pull fluorophores in the ground state has received much less attention, and the few existing examples focus on piezochromism of aggregates rather than on isolated molecular probes in hosts, such as lipid bilayer membranes.[10]

The planarization of oligothiophenes and related chromophores[11,12] without push–pull substituents has been studied extensively because of their intrinsic solvatochromism and thermochromism, and because of their promise in molecular electronics, photonics, and photovoltaics and as sensing devices. The responsiveness of oligothiophenes to the environment originates from the small energy cost for rotation around the α,α′-single bonds between two thiophene rings. Oligothiophenes with zero, one, or two adjacent methyl groups in β-position are planar in their excited state.[12] In the ground state, the α,α′-dihedral angle in the presence of one β-methyl group is 21° from *anti* conformation in the gas phase and 0° in the crystal. With two proximal β,β′-methyl groups, α,α′-dihedral angles in the crystal can vary from 0° to 30° and 46° from *anti* conformation. This variability of their dihedral angle promises high environmental responsiveness of β-methylated and β,β′-dimethylated fluorescent probes. Quite extensive computational data is available in support of these high expectations.[12] Herein, we show that moderately deplanarized, highly solvatochromic push–pull quaterthiophene scaffolds respond to decreasing membrane fluidity and increasing membrane potentials with a bathochromic shift (Figure 1). These findings suggest that both a confining surrounding and a stabilized macrodipole can planarize a twisted chromophore.

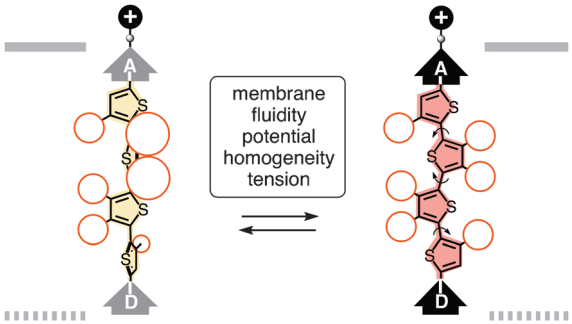

Figure 1. The coupling of fluorophore deplanarization by lateral crowding along the scaffold (red circles) and fluorophore polarization by terminal donors (D), acceptors (A), and charges (+) is proposed to provide conceptually innovative membrane probes.

Pertinent reports on push–pull oligothiophenes suggested that the quaterthiophene level would be ideal to begin with.[7] A partially deplanarized scaffold with one methyl group in β-position[12] and a methoxy donor at one terminus were selected as constants. π Acceptors were varied, covering cyanovinyl groups in compounds **1**–**3**, hydrazones in **4** and **5**, an aldehyde in **6**, and an ester in **7** (Scheme 1). To assure the amphiphilicity needed for delivery, partitioning, and orientation in lipid bilayers, we envisioned a covalent capture strategy that has been introduced recently to prepare otherwise intractable molecules with unusual physical properties in situ, such as the final amphiphiles **1**, **2**, **4**, and **5** (Scheme 1).[13] Monovalent, singly charged oximes and hydra-

[*] A. Fin, A. Vargas Jentzsch, Dr. N. Sakai, Prof. S. Matile
Department of Organic Chemistry, University of Geneva
Geneva (Switzerland)
E-mail: stefan.matile@unige.ch
Homepage: http://www.unige.ch/sciences/chiorg/matile/

[**] We thank D. Bassani (Bordeaux) and E. Vauthey (Geneva) for advise, D. Jeannerat, A. Pinto, and S. Grass for NMR measurements, the Sciences Mass Spectrometry (SMS) platform for mass spectrometry services, and the University of Geneva, the European Research Council (ERC Advanced Investigator), the National Centre of Competence in Research (NCCR) in Chemical Biology, and the Swiss NSF for financial support.

Supporting information for this article is available on the WWW under http://dx.doi.org/10.1002/anie.201206446.

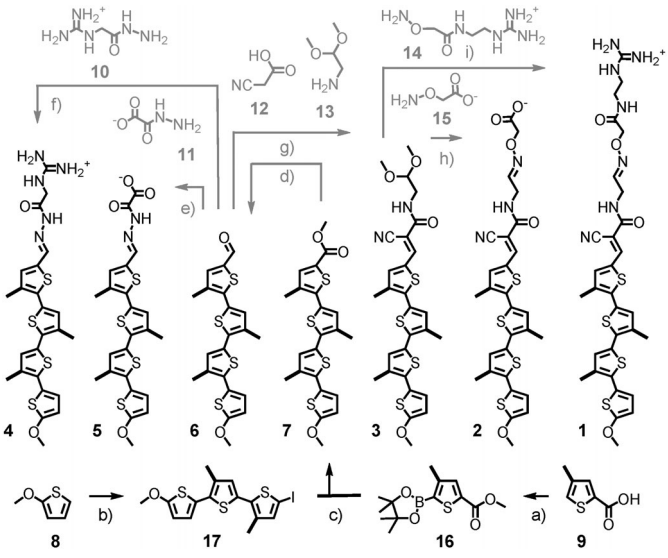

Scheme 1. Synthesis of planarizable push–pull probes. a) 1. H_2SO_4, MeOH, 16 h, 70 °C, 94 %; 2. $[Ir(cod)MeO]_2$ (cod = cycloocta-1,5-diene), 4,4′-di-*tert*-butyl-2,2′-bipyridine (dtbpy), bis(pinacolato)diboron, octane, 2 h, 70 °C, 90 %. b) 1. *N*-Iodosuccinimide (NIS), CH_2Cl_2, AcOH, 4.5 h, 0 °C to RT, 89 %; 2. 4,4,5,5-tetramethyl-2-(3-methylthiophen-2-yl)-1,3,2-dioxaborolane, $[Pd(PPh_3)_4]$, CsF, DMF, 16 h, 80 °C, 72 %; 3. as in (b) 1.), 88 %; 4. as in (b) 2.), 71 %; 5. as in (b) 1.), 45 %. c) $[Pd(PPh_3)_4]$, CsF, DMF, 16 h, 80 °C, 67 %. d) 1. Diisobutylaluminum hydride (DIBAL), CH_2Cl_2, MeOH, 2 h, −78 °C, 70 %; 2. MnO_2, CH_2Cl_2, 15 min, RT, 71 %. e) DMSO, AcOH, 60 °C, 3 h, 80 %. f) As in (e), quant. g) 1. **12**, piperidine, CH_3CN, 4 h, 70 °C, 63 %; 2. **13**, *O*-(1*H*-benzotriazoyl-1-yl)-*N*,*N*,*N*′,*N*,′-tetramethyluronium hexafluorophosphate (HBTU), triethylamine (TEA), DMF, 1.5 h, RT, 85 %. h) 1. TsOH·H_2O, CH_2Cl_2, 15 h, RT, 54 %; 2. DMSO, AcOH, 60 °C, 1 h, quant. i) As in (h).

Table 1: Spectroscopic data of planarizable push–pull probes.

Cpd[a]	λ_{abs}[b] [nm]	$\Delta\lambda_{abs}$[c] [nm]	ε[d] [$M^{-1}cm^{-1}$]	λ_{em}[e] [nm]	$\Delta\lambda_{em}$[f] [nm]	Φ_f[g] [%]	μ_e[h] [D]
1	480	26	17300	679	132	5	17
2	468	15	16900	680	130	10	15
3	476	18	19900	717	115	46	19
4	427	23	16200	551	39	7	9
5	434	8	16700	588	50	8	8
6	426	16	17400	629	89	31	14
7	407	11	20800	555	36	8	12

[a] Compounds, see Scheme 1. [b] Absorption maxima in chloroform. [c] Shift of absorption maxima from hexane to chloroform. [d] Extinction coefficient. [e] Emission maxima in chloroform. [f] Shift of emission maxima from hexane to chloroform. [g] Fluorescence quantum yields in chloroform. [h] Excited-state dipole moment, from Bakhishiev–Kawski (Figure S27 in the Supporting Information).

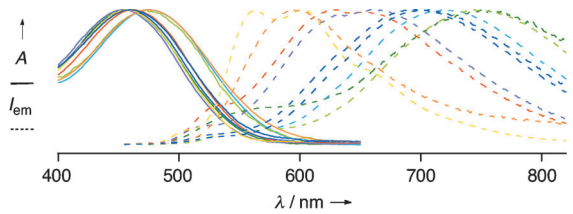

Figure 2. Absorption (solid) and emission (dotted) spectra of **3** in, with increasingly red-shifted emission, hexane (yellow), 2,2,2-trifluoroethanol (TFE; orange), dioxane (red), diethyl ether (light purple), ethyl acetate (deep purple), THF (blue), chloroform (cyan), acetone (dark green) and dichloromethane (light green).

zones were selected to avoid complications from multivalency. Slight differences in length were considered irrelevant because, in action, these hydrophilic termini are expected to float freely above the lipid bilayer.

Aldehyde **6**, the key intermediate, was synthesized by using routine Suzuki coupling procedures from methoxythiophene **8** for initiation and carboxylic acid **9** for termination (Scheme 1 and Scheme S1 and Figures S1–S20 in the Supporting Information). Amphiphiles **4** and **5** could be obtained in situ from **6** by incubation with the hydrazides **10** and **11**, respectively. Amphiphiles **1** and **2** were prepared from **6** by Knoevenagel condensation with **12**, amide formation with **13**, and deprotection of **3** before incubation with alkoxyamines **14** and **15**, respectively.

The absorption spectra of push–pull probes **1**–**7** in chloroform showed the best red shifts with the most powerful cyanovinyl acceptors in **1** (λ_{max} = 480 nm, Figures S21–S26 in the Supporting Information; Table 1 and Tables S1 and S2 in the Supporting Information). Similar shifts were found for the anionic **2** and the neutral **3**. Aldehyde and hydrazone acceptors gave weaker shifts around λ_{max} ca. 427 nm; esters were weakest at λ_{max} = 407 nm.

Identical trends but more dramatic effects were found in the emission spectra (Figure 2, Figures S21–S26 in the Supporting Information; Table 1, Tables S1–S3 in the Supporting Information). In chloroform, cyanovinyl acceptors in **1**–**3** gave the most impressive shifts to λ_{max} = 679–717 nm, whereas hydrazones **4** and **5** and ester **7** emitted already at λ_{max} = 551–588 nm. The dependence of the Stokes shifts on the solvent polarity functions from Bakhishiev–Kawski gave the exited-state dipole moments μ_e (Table 1, Tables S4 and S5 and Figure S27 in the Supporting Information).[14] The μ_e = 14 D obtained for aldehyde **6** dropped to $\mu_e \leq 9$ D upon transformation into hydrazones **4** and **5**. These results confirmed that hydrazones are poor π acceptors because of the "back-donating" aza-enamine motif. The same rational explained why hydrazone protonation is ineffective to recover push–pull strength.

The strongest μ_e = 19 D was found with cyanovinyl groups in **3**. The value did not change much with the introduction of terminal charges in **1** and **2** with more remote oxime bridges (Table 1). In chloroform, terminal charges strongly reduced the fluorescence quantum yield of the neutral fluorophores **3** (Φ_f = 46 %) and **6** (Φ_f = 31 %, Table 1), presumably owing to aggregation of the amphiphiles. The influence of fixed charges on the properties of planarizable push–pull fluorophores in general is interesting and deserves further investigation, particularly in the context of lipid bilayers.[2,4]

Absolute HOMO and LUMO energy levels were determined by cyclic voltammetry (Figure S37 and Table S7 in the Supporting Information). The obtained HOMO and LUMO energies −5.42 eV and −3.56 eV for **3** were in the expected range. Weaker π acceptors gave higher LUMO energies, whereas HOMO energies remained unchanged.[7,11]

To probe for membrane fluidity, the planarizable push–pull oligothiophene **1** was added to large unilamellar vesicles (LUVs) composed of dipalmitoyl phosphatidylcholine (DPPC). At 41 °C, DPPC membranes undergo a reversible transition from gel to fluid phase.[15] Upon cooling from 55 to 25 °C, the excitation maximum of probe **1** in DPPC LUVs shifted from $\lambda_{max} = 467$ nm to $\lambda_{max} = 487$ nm, that is $\Delta\lambda_{max} = 20$ nm (879 cm^{-1}) to the red (Figure 3b). Heating to 55 °C shifted the maximum back to $\lambda_{max} = 467$ nm, cooling again to 25 °C reproduced the shift to $\lambda_{max} = 487$ nm, and so on for continuing heating–cooling cycles (Figure 3c, ●). Concentration independence down to 0.1 mol % **1** in DPPC implied that the observed shifts do not originate from probe aggregation in the membrane. The excitation maximum in gel-phase DPPC exceeded all maxima measured for **1** in different solvents (Figure 2, Table S2 in the Supporting Information).

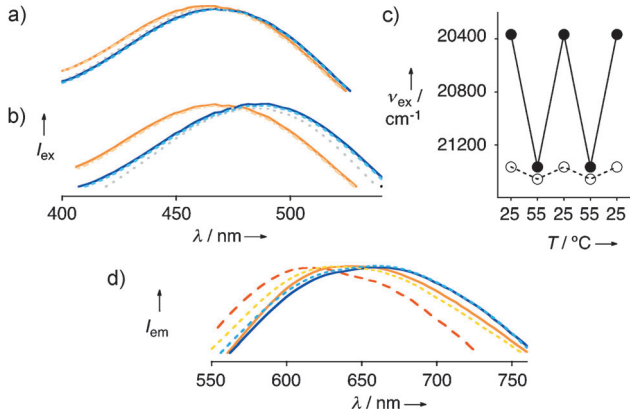

Figure 3. a, b) Excitation spectra of **1** in DOPC (a) and DPPC vesicles (b) at 25 °C (blue) and 55 °C (gold) for several heating–cooling cycles. The spectra in (a, b) have the same *x*-axis, but the spectra in (a) are shifted up along the *y*-axis for clarity. c) Excitation maximum of **1** during heating–cooling cycles in DOPC (○) and DPPC (●). d) Emission spectra of **1** added to DPPC vesicles at 25 °C (red, dashed), heated to 55 °C (solid, gold), cooled to 25 °C (solid, blue), heated to 55 °C (dotted, gold), and cooled to 25 °C (dotted, cyan).

The emission spectra were much less affected by the change in membrane phase (Figure 3d). Addition of **1** to DPPC LUVs at 25 °C gave a blue-shifted emission at λ_{max} ca. 610 nm (Figure 3d, dashed, red) that moved to λ_{max} ca. 650 nm after heating to 55 °C (Figure 3d, solid, gold) and remained there while cooling back to 25 °C (Figure 3d, solid, blue). This observation revealed, firstly, that partitioning into gel-phased DPPC is hindered and, secondly, that the transition from fluid to gel phase does not eject the oligothiophene probe. The compatibility of planarizable push–pull probes with crystalline membranes is interesting, because it is contrary to many examples in the literature.[16] Negligible shifts in emission observed upon further heating–cooling cycles indicated that the changes found in the excitation spectra do not originate from solvatochromism, that is, changes of the polarity of the environment during heating–cooling cycles (Figure 3d, solid and dotted).

Unlike DPPC, membranes composed of dioleoyl phosphatidylcholine (DOPC) remain in the fluid phase also at 25 °C. No significant shifts as in DPPC LUVs were observed during heating–cooling cycles in DOPC LUVs (Figure 3a, c, ○). This contrast supported that the oligothiophene chromophore is indeed planarized in gel-phase DPPC.[17] Nearly identical red shifts with probes **1**, **2**, **4**, and **5** indicated that their planarization by lateral confinement in crystalline membranes is independent of the polarization of the push–pull chromophores (Figures S28–S32 in the Supporting Information).[18]

Membrane potentials were applied to EYPC vesicles by connecting potassium gradients with valinomycin (Figure S33 and Table S6 in the Supporting Information, EYPC = egg yolk phosphatidylcholine).[4] With increasingly polarized vesicles, a bathochromic shoulder appeared in the excitation spectrum of the cationic probe **1** (Figure 4b). This shoulder at $I_{ex(50)}$ (that is, 50 % of maximal excitation intensity) widened with increasing polarization, resulting in a maximal red shift of $\Delta\lambda = 17$ nm (594 cm^{-1}, Figure 4b, c). Fluorescence kinetics measured at $\lambda_{ex(530)}$ (that is, the excitation wavelength of highest sensitivity) reported the build-up of membrane potentials in response to the addition of valinomycin and the instantaneous depolarization in response to lysis with melittin (Figure 4d).

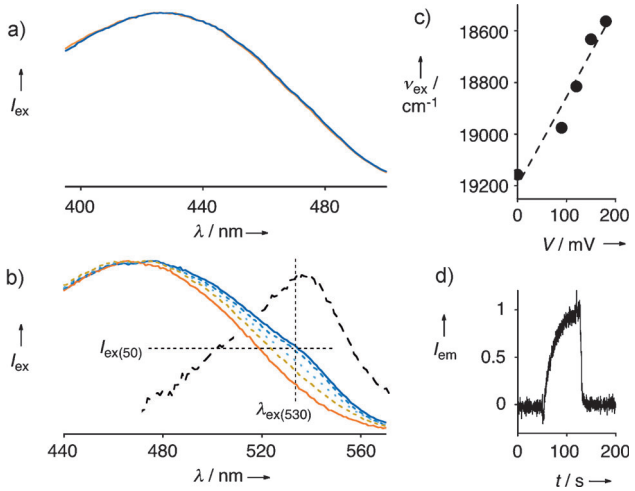

Figure 4. a) Excitation spectra of **4** in EYPC vesicles without (0 mV, gold) and with membrane potential (−180 mV, blue, $\lambda_{em} = 630$ nm). b) Same spectra as in (a) for **1** at, with increasing red shift, 0 (solid, gold), −90, −120, −150, and −180 mV (solid, blue, $\lambda_{em} = 600$ nm), and difference spectra for full against zero polarization (dashed, black). c) Red shift in the $I_{ex(50)}$ of **1** as a function of the applied membrane potential. d) Emission of **1** at $\lambda_{em} = 630$ nm ($\lambda_{ex} = 530$ nm) during the addition of valinomycin (1 μM, at 60 s) and melittin (2 μM, at 130 s) to EYPC LUVs with inside 100 mM KCl and outside 100 mM MCl (M = Na/K 1124:1), 10 mM tris(hydroxymethyl)aminomethane hydrochloride (Tris), pH 7.

Weaker shifts were found with the anionic probe **2**, and the cationic probe **4** was totally insensitive to membrane potentials (Figure 4a, Figures S34–S36 in the Supporting Information). Moreover, the shape of emission spectra was almost insensitive to membrane potentials in all cases.

Weakened voltage sensitivity with reduced push–pull strength and nearly voltage-independent emission were both consistent with the idea that fluorophore planarization by dipole-potential interactions can be used to sense membrane potentials.[19] The complementary independence of the response to membrane fluidity on the push–pull strength of the fluorophore provided further support for this conclusion. With decreasing fluidity, fluorophore planarization is expected to originate from increasing lateral confinement rather than from dipole-potential interactions. Although the complexity of the system suggests that alternative explanations should not be fully excluded at this stage, these initial results on a new topic are in perfect agreement with expectations, provide clear guidelines for the continuation, and promise attractive applications. Specifically, we now try to first maximize sensitivity and contrast with increasingly twisted, polarized, shortened, or elongated oligothiophenes,[19] and then to explore the detectability of membrane tension[20] or heterogeneity ("rafts")[3] together with applications toward live cells (neurons, etc)[3,5] and functional materials (artificial photosystems,[21] piezochromism,[10] NLO, etc).

Received: August 10, 2012
Revised: October 17, 2012
Published online: November 5, 2012

Keywords: fluorescent probes · membrane potential · oligothiophenes · torsion angle · vesicles

[1] a) M. Cianci, P. J. Rizkallah, A. Olczak, J. Raftery, N. E. Chayen, P. F. Zagalsky, J. R. Helliwell, *Proc. Natl. Acad. Sci. USA* **2002**, *99*, 9795 – 9800; b) B. Baumeister, S. Matile, *Chem. Eur. J.* **2000**, *6*, 1739 – 1749.

[2] a) M. Sheves, K. Nakanishi, B. Honig, *J. Am. Chem. Soc.* **1979**, *101*, 7086 – 7088; b) R. Rajamani, Y.-L. Lin, J. Gao, *J. Comput. Chem.* **2011**, *32*, 854 – 865.

[3] a) T. Baumgart, G. Hunt, E. R. Farkas, W. W. Webb, G. W. Feigenson, *Biochim. Biophys. Acta Biomembr.* **2007**, *1768*, 2182 – 2194; b) H. M. Kim, B. R. Cho, *Acc. Chem. Res.* **2009**, *42*, 863 – 872; c) L. A. Bagatolli, *Biochim. Biophys. Acta Biomembr.* **2006**, *1758*, 1541 – 1556; d) O. A. Kucherak, S. Oncul, Z. Darwich, D. A. Yushchenko, Y. Arntz, P. Didier, Y. Mely, A. S. Klymchenko, *J. Am. Chem. Soc.* **2010**, *132*, 4907 – 4916; e) E. W. Miller, J. Y. Lin, E. P. Frady, P. A. Steinbach, W. B. Kristan, Jr., R. Y. Tsien, *Proc. Natl. Acad. Sci. USA* **2012**, *109*, 2114 – 2119.

[4] a) N. Sakai, D. Houdebert, S. Matile, *Chem. Eur. J.* **2003**, *9*, 223 – 232; b) N. Sakai, S. Matile, *J. Am. Chem. Soc.* **2002**, *124*, 1184 – 1185; c) N. Sakai, D. Gerard, S. Matile, *J. Am. Chem. Soc.* **2001**, *123*, 2517 – 2524; d) N. Sakai, S. Matile, *Chem. Eur. J.* **2000**, *6*, 1731 – 1737; e) J.-Y. Winum, S. Matile, *J. Am. Chem. Soc.* **1999**, *121*, 7961 – 7962.

[5] P. Yan, A. Xie, M. Wei, L. M. Loew, *J. Org. Chem.* **2008**, *73*, 6587 – 6594.

[6] M. Zambianchi, F. Di Maria, A. Cazzato, G. Gigli, M. Piacenza, F. Della Sala, G. Barbarella, *J. Am. Chem. Soc.* **2009**, *131*, 10892 – 10900.

[7] a) S. Rodríguez González, J. Orduna, R. Alicante, B. Villacampa, K. A. McGee, J. Pina, J. Seixas de Melo, K. M. Schwaderer, J. C. Johnson, B. A. Blackorbay, J. J. Hansmeier, V. F. Bolton, T. J. Helland, B. A. Edlund, T. M. Pappenfus, J. T. López Navarrete, J. Casado, *J. Phys. Chem. B* **2011**, *115*, 10573 – 10585; b) H. Bürckstümmer, E. V. Tulyakova, M. Deppisch, M. R. Lenze, N. M. Kronenberg, M. Gsänger, M. Stolte, K. Meerholz, F. Würthner, *Angew. Chem.* **2011**, *123*, 11832 – 11836; *Angew. Chem. Int. Ed.* **2011**, *50*, 11628 – 11632; c) F. Effenberger, F. Würthner, *Angew. Chem.* **1993**, *105*, 742 – 744; *Angew. Chem. Int. Ed. Engl.* **1993**, *32*, 719 – 721; d) E. E. Nesterov, J. Skoch, B. T. Hyman, W. E. Klunk, B. J. Bacskai, T. M. Swager, *Angew. Chem.* **2005**, *117*, 5588 – 5592; *Angew. Chem. Int. Ed.* **2005**, *44*, 5452 – 5456.

[8] J. Shao, S. Ji, X. Li, J. Zhao, F. Zhou, H. Guo, *Eur. J. Org. Chem.* **2011**, 6100 – 6109.

[9] H.-J. Yoon, M. Dakanali, D. Lichlyter, W. M. Chang, K. A. Nguyen, M. E. Nipper, M. A. Haidekker, E. A. Theodorakis, *Org. Biomol. Chem.* **2011**, *9*, 3530 – 3540.

[10] F. Chen, J. Zhang, X. Wan, *Chem. Eur. J.* **2012**, *18*, 4558 – 4567.

[11] a) P. van Rijn, D. Janeliunas, A. M. A. Brizard, M. C. A. Stuart, R. Eelkema, J. H. van Esch, *Chem. Eur. J.* **2010**, *16*, 13417 – 13428; b) I. O. Shklyarevskiy, P. Jonkheijm, P. C. M. Christianen, A. P. H. J. Schenning, E. W. Meijer, O. Henze, A. F. M. Kilbinger, W. J. Feast, A. Del Guerzo, J.-P. Desvergne, J. C. Maan, *J. Am. Chem. Soc.* **2005**, *127*, 1112 – 1113; c) A. Mishra, C. Ma, P. Bäuerle, *Chem. Rev.* **2009**, *109*, 1141 – 1276; d) Y. Ie, A. Han, T. Otsubo, Y. Aso, *Chem. Commun.* **2009**, 3020 – 3022; e) I. Osaka, R. D. McCullough, *Acc. Chem. Res.* **2008**, *41*, 1202 – 1214; f) H. S. O. Chan, C. Ng, *Prog. Polym. Sci.* **1998**, *23*, 1167 – 1231; g) B. Jousselme, P. Blanchard, N. Gallego-Planas, J. Delaunay, M. Allain, P. Richomme, E. Levillain, J. Roncali, *J. Am. Chem. Soc.* **2003**, *125*, 2888 – 2889; h) M. Leclerc, *Adv. Mater.* **1999**, *11*, 1491 – 1498.

[12] G. Macchi, B. Milián Medina, M. Zambianchi, R. Tubino, J. Cornil, G. Barbarella, J. Gierschner, F. Meinardia, *Phys. Chem. Chem. Phys.* **2009**, *11*, 984 – 990.

[13] J. Montenegro, E.-K. Bang, N. Sakai, S. Matile, *Chem. Eur. J.* **2012**, *18*, 10436 – 10443.

[14] B. Siddlingeshwar, S. M. Hanagodimath, *Spectrochim. Acta Part A* **2009**, *72*, 490 – 495.

[15] R. Koynova, M. Caffrey, *Biochim. Biophys. Acta Rev. Biomembr.* **1998**, *1376*, 91 – 145.

[16] S. Otto, M. Osifchin, S. L. Regen, *J. Am. Chem. Soc.* **1999**, *121*, 10440 – 10441.

[17] In vesicle-free water, all amphiphiles were not fluorescent.

[18] Negligible shifts of emission/excitation maxima and decreasing emission intensity were found for **1** in response to increasing viscosity (glycerol/ethylene glycol mixtures).[8,9]

[19] Shortened terthiophene homologues remain sensitive to fluidity but are nearly insensitive to voltage, and the blue shift of more twisted quaterthiophene analogues is at least $\Delta\lambda = 60$ nm. These preliminary results support that more than general electrochromism accounts for the voltage sensitivity of **1** (e.g., planarization by macrodipole-potential interactions), and that the probes can be optimized for larger shifts before eventual applications to biological systems.

[20] A. Roux, K. Uyhazi, A. Frost, P. De Camilli, *Nature* **2006**, *441*, 528 – 531.

[21] N. Sakai, S. Matile, *J. Am. Chem. Soc.* **2011**, *133*, 18542 – 18545.

